Short-term variability in Greenland Ice Sheet motion forced by time-varying meltwater drainage: Implications for the relationship between subglacial drainage system behavior and ice velocity

Ian Bartholomew,[1] Peter Nienow,[1] Andrew Sole,[1] Douglas Mair,[2] Thomas Cowton,[1] and Matt A. King[3]

Received 22 September 2011; revised 17 May 2012; accepted 27 May 2012; published 7 July 2012.

[1] High resolution measurements of ice motion along a ~120 km transect in a land-terminating section of the GrIS reveal short-term velocity variations (<1 day), which are forced by rapid variations in meltwater input to the subglacial drainage system from the ice sheet surface. The seasonal changes in ice velocity at low elevations (<1000 m) are dominated by events lasting from 1 day to 1 week, although daily cycles are largely absent at higher elevations, reflecting different patterns of meltwater input. Using a simple model of subglacial conduit behavior we show that the seasonal record of ice velocity can be understood in terms of a time-varying water input to a channelized subglacial drainage system. Our investigation substantiates arguments that variability in the *duration* and *rate*, rather than absolute volume, of meltwater delivery to the subglacial drainage system are important controls on seasonal patterns of subglacial water pressure, and therefore ice velocity. We suggest that interpretations of hydro-dynamic behavior in land-terminating sections of the GrIS margin which rely on steady state drainage theories are unsuitable for making predictions about the effect of increased summer ablation on future rates of ice motion.

Citation: Bartholomew, I., P. Nienow, A. Sole, D. Mair, T. Cowton, and M. A. King (2012), Short-term variability in Greenland Ice Sheet motion forced by time-varying meltwater drainage: Implications for the relationship between subglacial drainage system behavior and ice velocity, *J. Geophys. Res.*, *117*, F03002, doi:10.1029/2011JF002220.

1. Introduction

[2] Mass loss from the Greenland Ice Sheet (GrIS) is one of the largest unknown components in predictions of future sea level change [*Meehl et al.*, 2007]. The ice sheet loses mass primarily through melting at its surface, which runs off, and discharge of icebergs to the ocean where glaciers meet the sea. Where the ice sheet terminates on land, ice flow velocities are enhanced each summer by meltwater which drains to the ice-bed interface, lubricating basal motion [*Zwally et al.*, 2002; *Van de Wal et al.*, 2008; *Joughin et al.*, 2008; *Bartholomew et al.*, 2010, 2011a; *Sundal et al.*, 2011]. Should there be a direct and positive relationship between the amount of meltwater produced and the magnitude of the seasonal increase in ice flow [*Zwally et al.*, 2002], this process has the potential to increase the rate of mass loss from the GrIS significantly in response to anticipated climate warming, by drawing ice to lower elevations where temperatures are warmer [*Parizek and Alley*, 2004]. While the impact of meltwater on fluctuations in ice flow has been a research focus for glaciologists studying Alpine and Arctic glaciers for decades [e.g., *Iken*, 1981; *Iken et al.*, 1983; *Iken and Bindschadler*, 1986; *Hooke et al.*, 1989; *Kamb et al.*, 1985; *Kamb*, 1987; *Mair et al.*, 2001; *Anderson et al.*, 2004; *Bartholomaus et al.*, 2007; *Bingham et al.*, 2008], the problem is now receiving renewed attention in the context of large ice sheet systems [*Zwally et al.*, 2002; *Van de Wal et al.*, 2008; *Joughin et al.*, 2008; *Das et al.*, 2008; *Shepherd et al.*, 2009; *Bartholomew et al.*, 2010; *Schoof*, 2010; *Pimentel and Flowers*, 2011; *Bartholomew et al.*, 2011b, 2011a; *Sundal et al.*, 2011], with the ultimate aim of reducing uncertainty in ice sheet models that are used to predict sea level change [*Parizek*, 2010].

[3] Meltwater influences rates of basal motion by altering effective pressure at the ice-bed interface, defined as ice overburden minus subglacial water pressure. Lower effective pressure (higher water pressure) favors faster sliding as it reduces drag between ice and the bed [*Iken and Bindschadler*, 1986].

[1]School of Geosciences, University of Edinburgh, Edinburgh, UK.
[2]School of Geosciences, University of Aberdeen, Aberdeen, UK.
[3]School of Civil Engineering and Geosciences, Newcastle University, Newcastle upon Tyne, UK.

Corresponding author: I. Bartholomew, School of Geosciences, University of Edinburgh, Drummond Street, Edinburgh, EH8 9XP, UK. (ian.bartholomew@ed.ac.uk)

0148-0227/12/2011JF002220

[4] One of the major controls on subglacial water pressure is the structure of the drainage system [*Röthlisberger*, 1972; *Walder*, 1986; *Röthlisberger and Lang*, 1987; *Schoof*, 2010] which, in turn, reflects the recent water flux [*Nienow et al.*, 1998]. Where overall water flux through the subglacial drainage system is low, a spatially distributed system with low capacity predominates [*Schoof*, 2010]. This is thought typically to comprise of one or more interactive components: interlinked cavities; drainage through sediments; and a thin meltwater film [e.g., *Hubbard and Nienow*, 1997]. These systems transmit water at relatively slow speeds and are often described as 'inefficient' [e.g., *Raymond et al.*, 1995]. In a distributed drainage system increased water flux leads to raised water pressures and therefore higher rates of basal sliding. When the subglacial water flux is raised, however, drainage conduits become enlarged by melting of their walls and efficient 'R-channels' develop [e.g., *Röthlisberger*, 1972]. In R-channels, higher rates of wall melting offset the closure of channel walls by the inward creep of ice, relieving water pressure in a way that is not possible where flux is low. Steady state analyses indicate that R-channels have an inverse pressure-discharge relationship; the largest channels which carry more water operate at lower pressure [*Röthlisberger*, 1972].Under conditions where meltwater drainage is steady or varies only gradually, therefore, a more efficient channelized subglacial drainage system is associated with higher effective pressure and reduced basal sliding [e.g., *Schoof*, 2010].

[5] As with Alpine systems, the drainage system in the ablation zone of the GrIS develops over the course of a melt season, from a spatially distributed inefficient system to a discrete network of efficient channels, in response to meltwater inputs from the ice sheet surface [*Nienow et al.*, 1998; *Bartholomew et al.*, 2011b]. Development of the drainage system occurs further from the ice sheet margin as the melt season progresses [*Bartholomew et al.*, 2011b]. Late summer ice velocities in marginal areas of the GrIS have been observed to be lower than in early summer, even while temperatures remain significantly above freezing, indicating that this drainage evolution acts to limit the overall magnitude of summer acceleration [*Bartholomew et al.*, 2010; *Sundal et al.*, 2011; *Bartholomew et al.*, 2011a; *Palmer et al.*, 2011].

[6] Consideration of the steady state theory of subglacial drainage, coupled with such observations from Greenland, has led a number of authors to suggest that increased surface melting will lead to a *reduction* in summer ice velocities in the GrIS compared with the present. It is argued that the transition from a predominantly inefficient drainage system to an efficient channelized one is critical in reducing the impact of meltwater drainage on ice velocity. If this transition occurs sooner each summer it may limit the time frame over which high water pressures (and therefore ice velocities) can occur [*Joughin et al.*, 2008; *Van de Wal et al.*, 2008; *Schoof*, 2010; *Pimentel and Flowers*, 2011; *Sundal et al.*, 2011].

[7] Subglacial conduits adjust in size to accommodate variations in meltwater discharge over timescales of days or more [e.g., *Röthlisberger*, 1972; *Spring*, 1980; *Röthlisberger and Lang*, 1987; *Cutler*, 1998; *Schoof*, 2010], while meltwater delivery can vary significantly over much shorter periods. It is unlikely, therefore, that steady state conditions ever exist in reality [*Röthlisberger*, 1972]. Temporary imbalance between the volume of water delivered to a subglacial drainage system and its ability to evacuate that water are accommodated by temporary spikes in subglacial water pressure *even once the drainage system has become more efficient* [*Röthlisberger and Lang*, 1987; *Schoof*, 2010].

[8] This raises a possible alternative explanation for ice velocity enhancement in land-terminating margins of the GrIS: that a large part of the seasonal ice motion signal may result from the aggregation of short-term speed-up events which are caused by overfilling of the drainage system in response to time-varying inputs of meltwater. Using this logic, it has been suggested that the discrepancy between early and late summer ice velocities in the GrIS [*Bartholomew et al.*, 2010; *Sundal et al.*, 2011; *Bartholomew et al.*, 2011a] occurs because over-pressurized conditions are common on the rising limb of seasonal meltwater production, regardless of drainage system structure, as the system is constantly challenged to evacuate larger quantities of water than before [*Bartholomew et al.*, 2011a]. The late summer decline in ice velocities is due, then, to a decline or stabilization of water input. This allows the subglacial drainage system to adjust to accommodate the water at lower pressures. In this scenario, development of a more efficient drainage system would be a prerequisite for the late summer decline in ice velocity, but is not sufficient to cause a drop in subglacial water pressure without a reduction in meltwater input relative to the capacity of the system.

[9] The purpose of this paper is to provide a reassessment of the role of drainage system behavior in mediating the relationship between meltwater and ice velocity in land-terminating sections of the GrIS margin. In the first part of the paper, we present high temporal resolution ice velocity measurements, derived from global position system (GPS) observations, along a land-terminating transect at ~67°N in western Greenland during the 2009 and 2010 melt seasons (Figure 1). These data are calculated from the same GPS data set that has been used in previous studies of Leverett Glacier which present ice velocity from Leverett Glacier as daily displacements [e.g., *Bartholomew et al.*, 2011a]. The higher resolution ice motion record is compared with in situ observations of air temperatures, as well as with proglacial hydrological data from the Leverett Glacier catchment which overlaps the lowest three sites (Figure 1) [*Bartholomew et al.*, 2011b]. The ice motion data reveal the detailed structure of ice velocity variations which make up the seasonal velocity signal, allowing us to investigate the relationship between variations in meltwater input and ice velocity on shorter timescales than previously. In the second part of the paper, we use a simple model of the behavior of a subglacial conduit to assess whether the features of the ice motion signal can be explained as a response of subglacial water pressure to time-varying water input.

2. Field Site and Previous Studies

[10] The key features of the seasonal ice velocity signal along this transect have been identified in two previous studies which used the same GPS observations to derive daily ice velocities from the summers of both 2009 and 2010 [*Bartholomew et al.*, 2011a; *Sole et al.*, 2010]. Measurements were made at 7 sites up to 1716 m elevation, which is ~115 km inland from the GrIS margin (Figure 1). The lowest

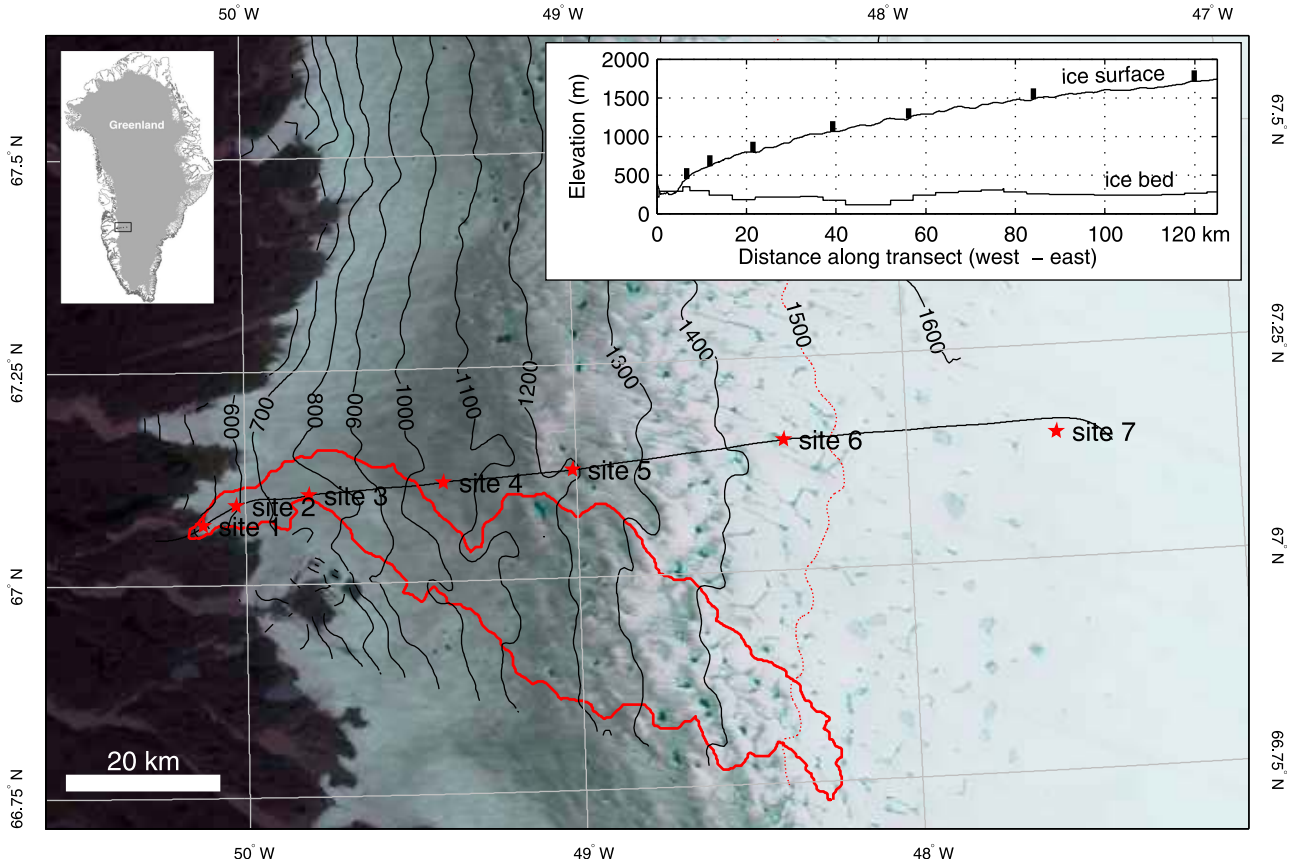

Figure 1. Map showing the location of the transect on the western margin of the GrIS. The sites where GPS and temperature measurements were made are indicated by red stars and the hydrological catchment of the proglacial river at Leverett Glacier is delineated in red. Contours are produced from a digital elevation model (DEM) derived from InSAR [*Palmer et al.*, 2011]. The long-term ELA in the region is located at around 1500 m [*Van de Wal et al.*, 2005]. The ice sheet profile (inset) is derived from surface elevation data collected during an airborne geophysical survey in 2010 (black line) [*Krabill*, 2010] and bed elevation data which is sampled from a DEM of the whole ice sheet [*Bamber et al.*, 2001].

elevation site is located on Leverett Glacier and is approximately 2 km from the glacier terminus.

[11] All of the sites along the transect experienced summer acceleration, where ice velocities are raised above winter background rates, in both 2009 and 2010. Initial increases in ice velocity followed the onset of surface melting at each site, which occurred at progressively higher elevations through the summer (Figures 2–5) [*Bartholomew et al.*, 2011b]. The initiation of locally forced velocity variations was characterized by rapid horizontal acceleration which was coincident with uplift of the ice sheet surface. This is indicative of initial access of surface meltwaters to the ice-bed interface and is analogous to 'spring-events' widely reported from Alpine and High Arctic glaciers [e.g., *Iken*, 1981; *Mair et al.*, 2001; *Anderson et al.*, 2004; *Bingham et al.*, 2008]. At site 7 there was no surface uplift in 2009 and very little in 2010. The minor increase in ice velocity at this site is attributed to the effect of coupling to faster ice downglacier [*Bartholomew et al.*, 2011a].

[12] The highest daily ice velocities, which peaked at site 2 at over 500 m yr^{-1}, and greatest overall seasonal acceleration, were achieved at sites nearest the ice sheet margin [*Bartholomew et al.*, 2011a; *Sole et al.*, 2010]. At lower elevation sites, where melt rates are higher (Figures 2 and 4) and the ice is less thick (Figure 1), the initial increase in ice velocity closely follows the onset of surface melting. Ice velocities at these sites are higher in early summer than in late summer. This is explained by the development of an efficient subglacial drainage system, in response to abundant meltwater input from the ice sheet surface, which is able to evacuate larger discharge at lower pressures than earlier in the summer [*Bartholomew et al.*, 2011b, 2011a].

[13] At sites further inland, however, there is a greater delay between the onset of melting and ice acceleration as melt rates are lower and it takes longer to accumulate enough meltwater to penetrate through thicker ice to the bed [*Bartholomew et al.*, 2011a]. This delay between the onset of melting and drainage of water from the ice surface to its bed is responsible for the lower overall acceleration as it limits the time frame for velocity variations to occur [*Bartholomew et al.*, 2011a]. Accumulation and drainage of stored water in the form of supraglacial lakes may be particularly important in forcing a hydraulic connection between the ice sheet surface and its bed at higher elevations [*Bartholomew et al.*, 2011b, 2011a].

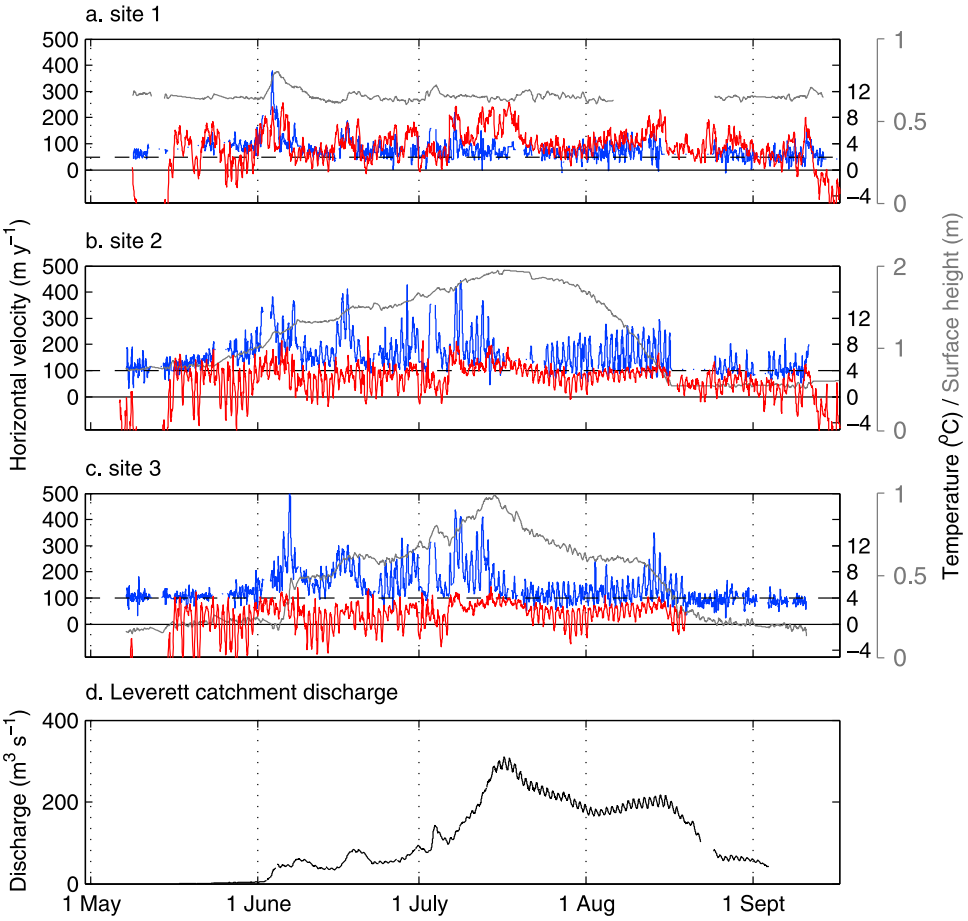

Figure 2. (a–c) Ice velocity (blue), surface height profile (grey) and air temperature (red) at sites 1–3 during the 2009 summer melt season. The surface height profile is shown relative to an arbitrary datum and has a linear, surface parallel, trend removed. Winter background ice velocity (black dashes) is determined from displacement of the GPS sites during winter 2009/2010. (d) Discharge from the Leverett Glacier proglacial river during the 2009 summer melt season.

[14] The seasonal development of the drainage system in the part of the ice sheet from which runoff drains through the Leverett Glacier snout (Figure 1, red outline) was also investigated in a hydrological study from 2009 [*Bartholomew et al.*, 2011b]. Observations of bulk hydrological parameters in the proglacial stream, coupled with a simple model of surface melting and satellite observations of supraglacial lake drainage, showed that an efficient drainage system developed progressively further inland from the ice sheet margin over the course of the melt season. This occurred in response to inputs of meltwater from the ice sheet surface [*Bartholomew et al.*, 2011b].

[15] Previous studies have found that longitudinal coupling is not effective over length scales of ~10 km along this transect on the basis that, in the early season, initial speed-up of the most marginal sites has little effect on ice motion further inland [*Bartholomew et al.*, 2010, 2011a]. Most sites exhibit slight speed-up, however, in the absence of surface uplift prior to the first major speed-up event of the summer. The most obvious example is site 2, which displays a short increase in velocity in the absence of any surface uplift between approximately May 5th–May 12th in 2010. This feature of the ice motion signal is likely due to coupling to faster moving ice further downglacier or either side of the transect [*Price et al.*, 2008; *Bartholomew et al.*, 2010, 2011a] albeit over relatively short distances. At the most marginal sites this longitudinal coupling phase lasts only for a matter of days, while at higher sites it can last from a few days up to a number of weeks [*Bartholomew et al.*, 2011a]. The minor acceleration at site 7 is also attributed to the effect of coupling to faster ice downglacier [*Bartholomew et al.*, 2011a]. We acknowledge, therefore, that some part of the velocity signal at each site is due to non-local forcing, however, the magnitude of the signal appears to be much smaller than velocity changes which are due to local hydrological forcing.

3. Data Collection and Methods

3.1. GPS Data

[16] We used dual-frequency Leica 500 and 1200 series GPS receivers to collect the season long records of ice motion at each site. Each GPS antenna was mounted on a pole drilled several meters into the ice, which subsequently froze in, providing measurements of ice motion that were independent of ablation. The GPS receivers collected data at 30 second intervals in 2009 and the first part of 2010. The data were

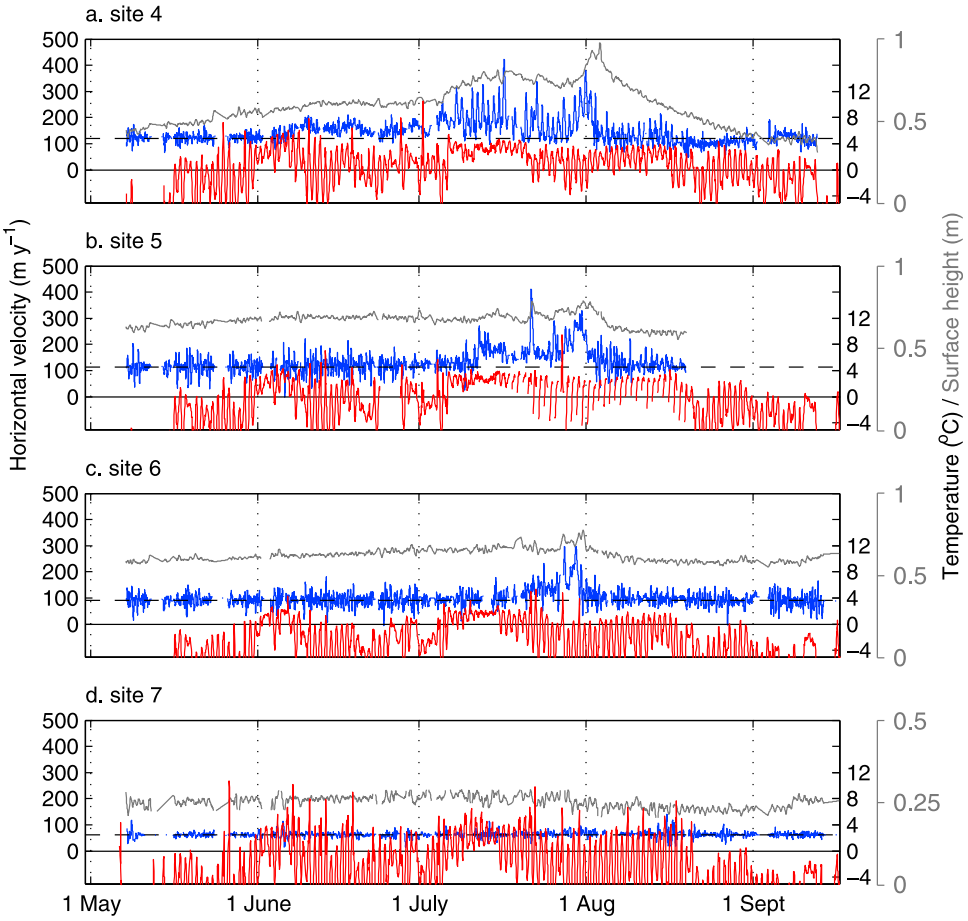

Figure 3. (a–d) Ice velocity (blue), surface height profile (grey) and air temperature (red) at sites 4–7 during the 2009 summer melt season. The surface height profile is shown relative to an arbitrary datum and has a linear, surface parallel, trend removed. Winter background ice velocity (black dashes) is determined from displacement of the GPS sites during winter 2009/2010.

processed using a kinematic approach relative to an off-ice base station at Kelyville, approximately 40 km west from the snout of Leverett Glacier, using the Track v1.21 software [*Chen*, 1999; *Herring et al.*, 2010]. In June 2010 we installed a new off-ice reference station less than 2 km from the Leverett Glacier snout, which collected data at 10 second intervals. Conservative estimates of the uncertainty associated with positioning at each epoch are approximately ± 1 cm in the horizontal direction and ± 2 cm in the vertical direction. The data were smoothed using a Gaussian low-pass filter to suppress high-frequency noise (<2 hours) without distorting the long-term signal. Short-term variations in ice velocity were derived by differencing positions at either end of a 6 hour sliding window, applied to the whole time series of filtered positions for each site. This window length was chosen in order to highlight short-term variations in the velocity records while retaining a high signal-to-noise ratio. Unfortunately, the quality of the GPS data at site 1 was compromised by technical problems, making it difficult to resolve short-term variations in horizontal velocity at this site. The surface height profiles that are presented have had a linear trend removed to account for surface parallel motion. Where we use the term 'uplift', therefore, this refers to upwards change in the detrended height profile.

[17] Uncertainties associated with the filtered positions are <0.5 cm in the horizontal and <1 cm in the vertical directions, corresponding to annual horizontal velocity uncertainties of <14.6 m yr^{-1} for the 6 hour velocity measurements. We used the standard deviation of the 6 hour sliding window velocities from site 7, which has the longest processing baseline and experienced negligible velocity variations, to estimate the noise floor in the GPS velocity records. The standard deviations for the 6 hour velocities at site 7 are 19.5 m yr^{-1}. These values compare well with the calculated uncertainties and represent conservative error estimates for our data set. The values for winter background ice-velocities are derived from the displacement of each GPS receiver between the end of the summer melt season and the following spring [*Bartholomew et al.*, 2010].

3.2. Air Temperate and Surface Ablation

[18] Simultaneous measurements of air temperature were made at each GPS site to constrain melt rates, and show that the velocity data cover the whole seasonal melt cycle. Measurements of air temperature were made using shielded Campbell Scientific T107 temperature sensors connected to Campbell Scientific CR800 data loggers (sites 1, 3 and 6) and shielded HOBO U21-004 temperature sensors (sites 2, 4, 5

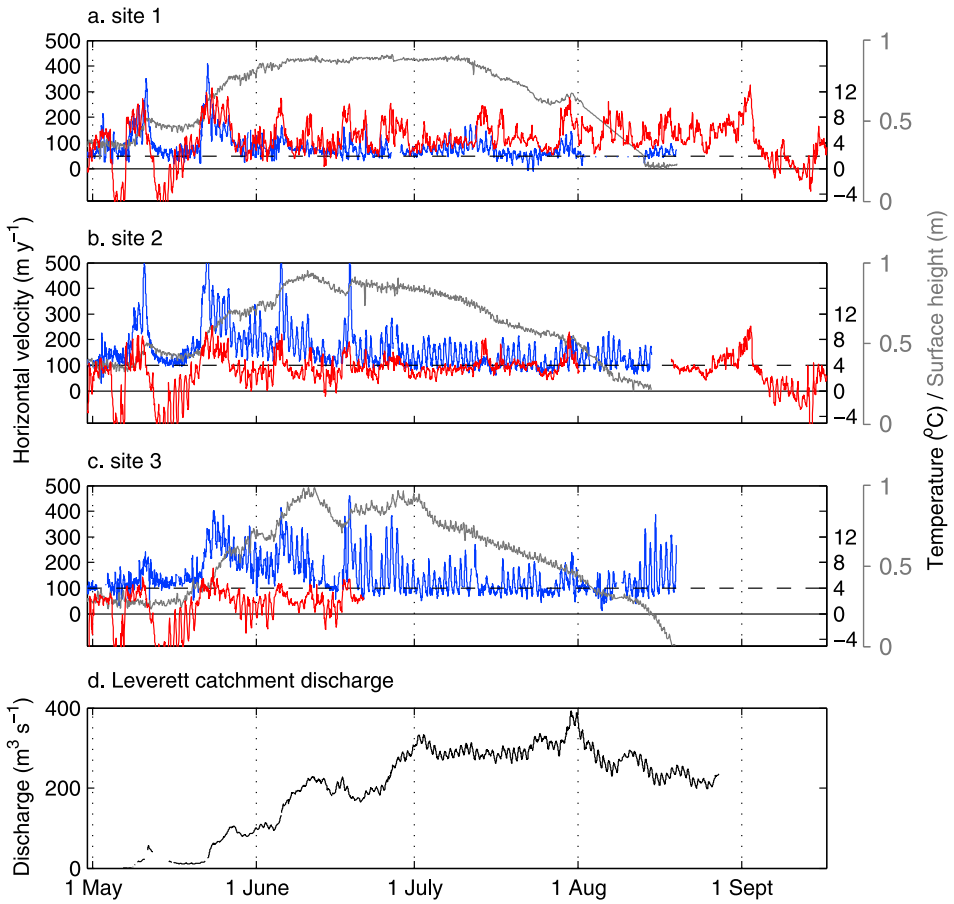

Figure 4. Same as Figure 2 for the 2010 melt season. Winter background ice velocity (black dashes) is determined from displacement of the GPS sites during winter 2009/2010.

and 7) at 15 minute intervals throughout the survey period. The temperature sensors were fixed to the same pole as the GPS antenna at each site meaning that the height of the sensor does not remain constant through the melt season. At sites with high levels of ablation, this led to changes in the sensor height relative to the ice surface of up to 2 m over the course of the summer. In order to assess how strongly this might influence measured air temperatures we used two sensors at different heights on the same pole (approx. 1 m apart) at site 1. Discrepancy between the records from these two sensors was small, suggesting that it is valid to compare temperatures through the melt season. Seasonal melt totals were also measured using ablation stakes at each GPS site.

3.3. Proglacial Discharge

[19] We made continuous measurements of water stage in the proglacial stream that emerges from the terminus of Leverett Glacier. Proglacial discharge was derived from a continuous stage-discharge rating curve calibrated with repeat dye dilution gauging experiments throughout the melt-season as described in *Bartholomew et al.* [2011b].

4. Observations

4.1. Short-Term Variations in Ice Velocity

[20] The higher temporal resolution ice motion records allow us to see changes in ice motion in much greater detail than in previous studies. At the sites nearest the margin, which lie within the Leverett Glacier hydrological catchment, the initial ice acceleration events are the most dramatic and coincide with the outburst of a pulse of meltwater from beneath the glacier (Figures 2 and 4). For example, at sites 1 and 2, velocities exceeded 400–500 m yr^{-1} in the 2010 spring event, which was coincident with a rise in proglacial discharge from less than 10 m^3 s^{-1} to 50 m^3 s^{-1} over three days.

[21] At sites 1–3, the spring-event follows a period of high temperatures and typically lasts a few days (up to a week), building to a sharp peak before velocities return to background levels. The decline in velocities that follows is coincident with leveling-off or a fall in discharge as well as a return to lower temperatures. Further inland, at the sites which lie outside the Leverett Glacier catchment, the initial locally forced velocity events are smaller (Figures 3 and 5). The uplift signal at sites 4–6 is more a change in trajectory than a steep rise, and velocities increase by 50–100 % rather than the 300–400 % observed at sites 1–3 (Figures 3 and 5). At these sites, the initial acceleration is also sustained for a longer period of time, without the marked drop-off back to winter levels.

[22] Following initial acceleration, the ice motion record from sites 1–3 is dominated by further short-term velocity variations on timescales ranging from a few hours to several days. Multiday speed-up events, which are characterized by

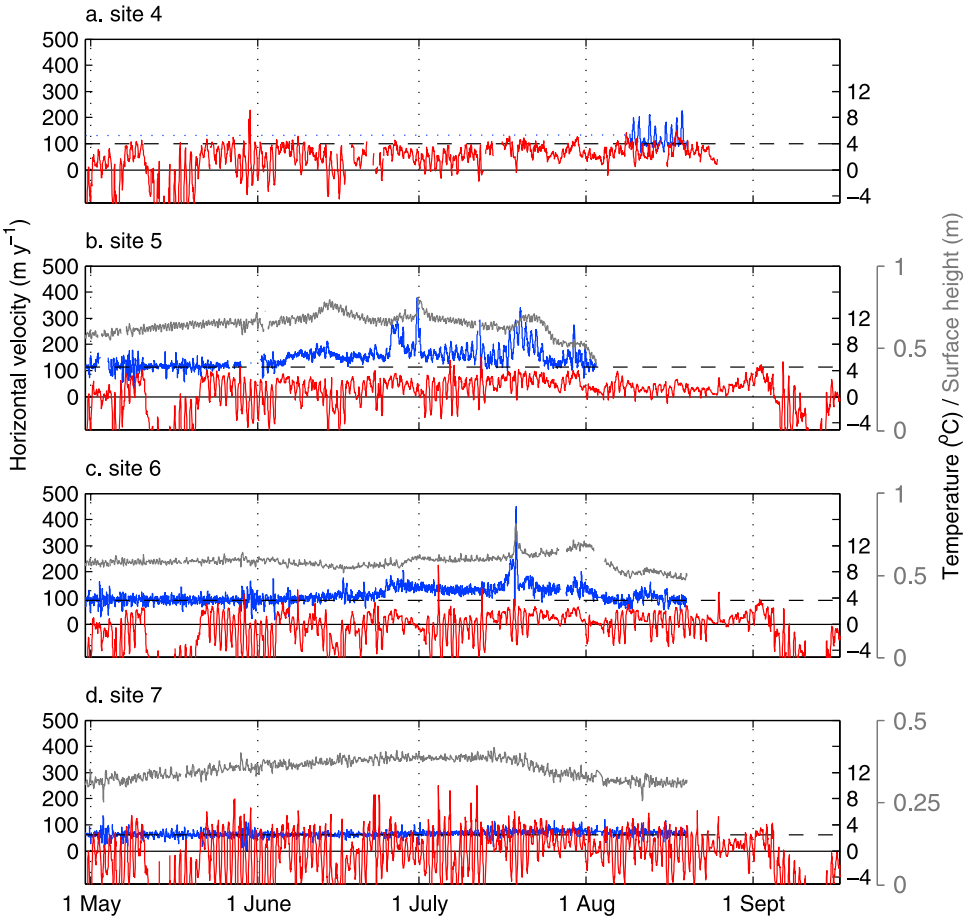

Figure 5. Same as Figure 3 for the 2010 melt season.

an increase in ice velocities lasting for more than a single day during which ice velocity does not return to background levels, occur at some point in the melt season at all sites except for site 7 in both 2009 and 2010 (Figures 2–5). Examples of such events occur in 2009 at sites 1–3, which all experience velocity increases of more than 100% between June 1st–June 10th. Similar events also occur at these sites in 2010 between May 20th–June 1st, and from June 4th–June 9th at sites 2 and 3. During these multiday events, ice velocity can increase by more than 200 m yr^{-1} within 24 hours (Figures 2 and 4) and does not return to background levels for an extended period. Multiday velocity events also occur at higher elevations in both 2009 and 2010. For example, at sites 4, 5 and 6 between July 23rd–August 1st in 2009, and at sites 5 and 6 from July 18th–24th in 2010.

[23] Without exception, these speed-ups are accompanied by uplift of the ice sheet surface by several centimeters. The most rapid surface uplift appears in conjunction with the most dramatic horizontal acceleration (Figures 2–5). At sites 1–3 these high velocity events are associated with steep rises in proglacial discharge, linking them to increased water flux through the subglacial drainage system. Strikingly, the surface height profiles of sites 2 and 3 in both 2009 and 2010 closely match the discharge curve measured at Leverett Glacier. The association is less clear at site 1, where the GPS data was of poorer quality, although the largest rises in discharge are still matched with uplift of the ice surface.

[24] The majority of the multiday events at sites 1–3 are associated with periods of raised temperatures which increase the volume of meltwater input to the subglacial drainage system for a short time (Figures 2 and 4). In some cases, however, ice velocities are raised for a number of days in the absence of high temperatures. For example, in 2009 velocities are raised at sites 1–3 between July 3rd –8th, which was a period of colder temperatures (Figure 2), although the event is still associated with ice surface uplift and a temporary increase in discharge at Leverett Glacier. One potential explanation is that strong winds which disrupt the boundary layer can be associated with high melt rates in the absence of high temperatures. A previous study found, however, that the hydrological signature of this meltwater pulse indicates drainage of large volumes of stored water from the ice sheet surface, which was delivered to the ice sheet margin via the ice-bed interface [*Bartholomew et al.*, 2011b], in a manner similar to the spring-events. The likely source for this water was identified, using satellite imagery, as a supraglacial lake within the Leverett Glacier catchment [*Bartholomew et al.*, 2011b].

[25] The highest velocity events at sites 4, 5 and 6 in both 2009 and 2010 are also not closely linked to warm air temperatures and we suggest that these are also caused by sudden drainage of stored water from the ice sheet surface. Satellite imagery from 2009 shows lake drainage events, where supraglacial ponds disappear from the ice sheet surface in

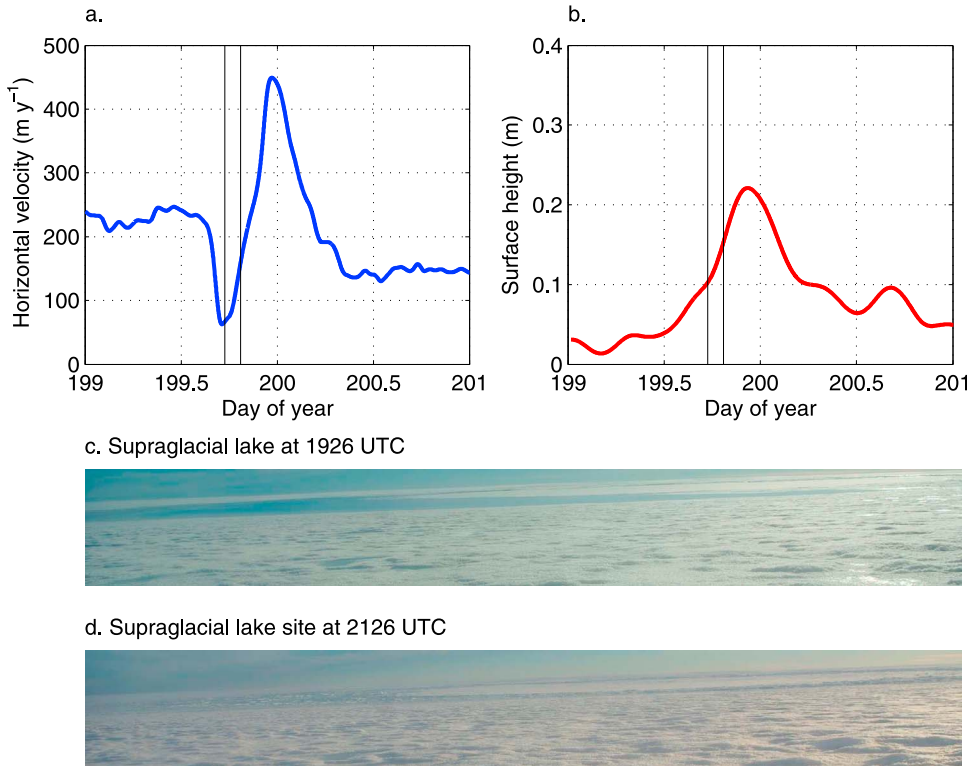

Figure 6. (a) Surface velocity at site 6 during the lake drainage event which occurred <2 km from the GPS receiver on July 18th 2010. (b) Surface height profile during the lake drainage event. (c and d) Before and after images of the supraglacial lake drainage event taken by a time lapse camera mounted on the support pole at site 6. The time at which the photos were taken is marked on the velocity and height profiles by vertical black lines.

consecutive images, in close proximity to these sites at times which correspond to the velocity events [*Bartholomew et al.*, 2011a]. Further, in 2010 we captured the rapid drainage of a lake which had accumulated less than 2 km from site 6 using time-lapse photography. Drainage of this lake coincided with a 400% increase in ice velocity on July 17th and uplift of the ice sheet surface of 0.3 m in less than 24 hours (Figure 6).

4.2. Diurnal Velocity Cycles

[26] The detailed velocity records also reveal clear daily cycles in ice motion at a number of the sites (Figures 2–5). These daily cycles are most clear at sites 2, 3 and 4 where their amplitude ranges from less than 50 m yr^{-1} to over 300 m yr^{-1}, ~300% of winter background rates. At these sites diurnal acceleration appears to be a dominant feature of the seasonal ice motion signal, particularly in the latter part of the melt season when longer-term increases in ice velocity are absent. They are also evident at site 1, although the relatively slow background velocity and technical problems with the GPS receiver mean that they are harder to resolve. In 2010, which was a significantly warmer year than 2009, daily cycles in ice velocity develop at site 5 from early July until the beginning of August. There are no discernible daily cycles in either year, however, at site 6 or 7.

[27] Daily cycles in ice velocity develop at sites 2–4 in 2009 following the beginning of locally forced acceleration. The behavior is very similar in 2010, although ice velocities are dramatically reduced at sites 1 and 2 after the spring-event due to a period of sub-freezing temperatures. When temperatures rise again, there is another multiday acceleration following which daily cycles begin. The daily velocity cycles at site 5 in 2010 develop later in the melt season, around June 24th, and their magnitude is from around 50–150 m yr^{-1}, slightly lower than those nearer the ice sheet margin. Once developed, these extremely rapid variations in ice velocity appear to be superimposed on the seasonal velocity signal, and, in the absence of other events, ice velocity consistently returns to around winter background rates on a diurnal basis (Figures 2–5). At sites 2 and 3 in 2009, for which we have the longest ice velocity and discharge records it is clear that the cycles become subdued when discharge rapidly declines after August 18th.

[28] Where daily cycles in ice velocity are evident, their timing is closely related to variations in both local temperatures and discharge from Leverett Glacier (Figure 7). Daily peaks in velocity lag the local temperature peak by 2–4 hours and this pattern is consistent across both years and between all of the sites which experience daily cycles. Although there is some variability in the lag between peak daily velocity and peak daily temperature, there is no discernible pattern in the relationship over the melt season. Previous studies found a similar delay and have suggested that this reflects a plausible transit time for supraglacial meltwater to collect and drain into the englacial drainage system before reaching the ice-bed interface [*Shepherd et al.*, 2009; *Bartholomew et al.*, 2011a]. By contrast with the temperature signal, daily peaks

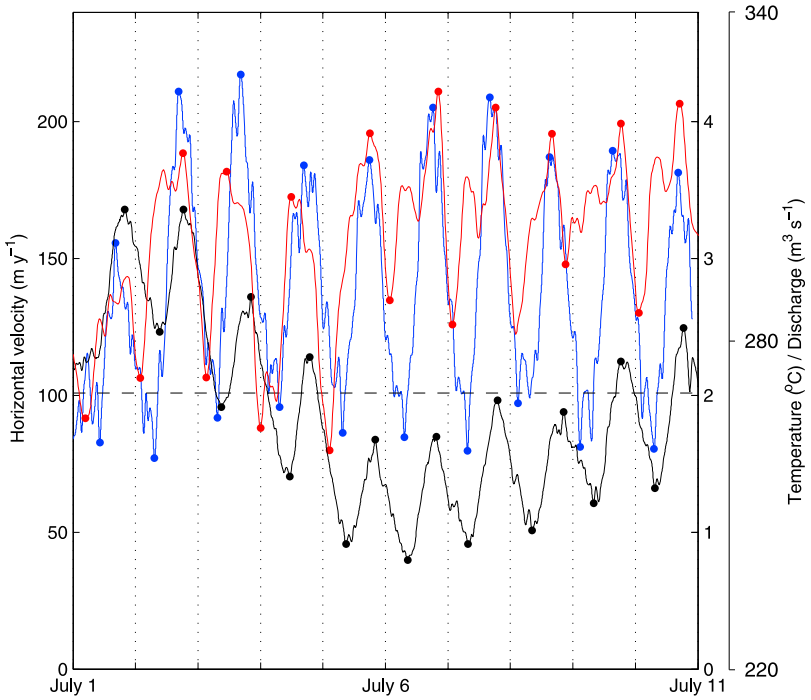

Figure 7. Detailed record showing the temporal relationship between diurnal cycles in ice velocity (blue), air temperature (red) and proglacial discharge (black) at site 2 between July 1 and July 10, 2010. Daily peaks and troughs are marked by colored dots. Winter background ice velocity is indicated by a black dashed line.

in ice velocity at sites 1, 2 and 3 precede the daily discharge peak at Leverett Glacier by 2.5, 1.6 and 1.2 hours on average respectively. This pattern is also consistent across both years and there is no seasonal signal. Daily velocity cycles at Site 4 in 2009 are almost in phase with discharge and at site 5 in 2010 the peak in ice velocity follows the peak in discharge. Since these sites lie outside of the Leverett Glacier hydrological catchment, however, there is little reason to imply cause and effect.

[29] Although we observe close relationships between the timing of variations, we can find no systematic relationship between the magnitude of the daily velocity cycles and daily range, peak or mean values in either temperature or discharge. Tentatively, we find the largest amplitude cycles in ice velocity at sites 2 and 3 in the early part of the melt season in both years, although there are some periods in the latter half of the season when the magnitude of daily velocity variations can still exceed 150% of winter background.

5. Subglacial Conduit Model

[30] The basic physical behavior of subglacial conduits can be described by a single equation for their cross-sectional area, S, which captures both cavity and R-channel behavior [*Schoof*, 2010]:

$$\frac{\partial S}{\partial t} = c_1 Q \frac{\partial \phi}{\partial s} + u_b h - c_2 N^n S \qquad (1)$$

where Q is the water discharge, $\frac{\partial \phi}{\partial s}$ is the hydraulic gradient along the conduit and $N = p_i - p_w$ is the effective pressure in the conduit (ice overburden, p_i, minus water pressure, p_w). The first term on the right-hand side in equation (1) is the rate of conduit opening due to wall melting, the second term is opening due to bed-parallel sliding (at speed u_b) past bedrock obstacles (with height h) and the third is conduit closure due to collapse under the weight of overlying ice. c_1 is a constant which is related to the latent heat of fusion for ice, L, by $c_1 = 1/(\rho_i / L)$, where ρ_i is the density of ice (910 kg m^{-3}). c_2 is equal to $2Bn^{-n}$ where B is Glen's flow law coefficient and $n = 3$ is the exponent in Glen's flow law for ice. Q can be related to S and $\frac{\partial \phi}{\partial s}$ by the Darcy-Weisbach law:

$$Q = \sqrt{\frac{8}{\rho_w f}} A^{3/2} \frac{\partial \phi}{\partial s}^{1/2} W^{-1/2} \qquad (2)$$

where A is the filled cross-sectional area, W is the channel wetted perimeter, ρ_w is the density of water (1000 kg m^{-3}) and f is the Darcy-Weisbach friction factor. Equation (2) is a general case of the equation which was applied by *Schoof* [2010] for a full semicircular conduit. Analysis of equation (1) by *Schoof* [2010] demonstrates, for steady state, that N decreases with Q below a critical threshold in Q, while at higher discharge N increases with Q, reflecting the transition from cavity to channel-like behavior.

[31] We present a simple model which uses equation (1) to describe the behavior of a subglacial conduit in a lumped formulation [e.g., *Clarke*, 1996, 2003] in response to time-varying water input. The configuration is inspired by the approach used by *Cutler* [1998]. In this model, a subglacial conduit is directly connected to a moulin that drains from the

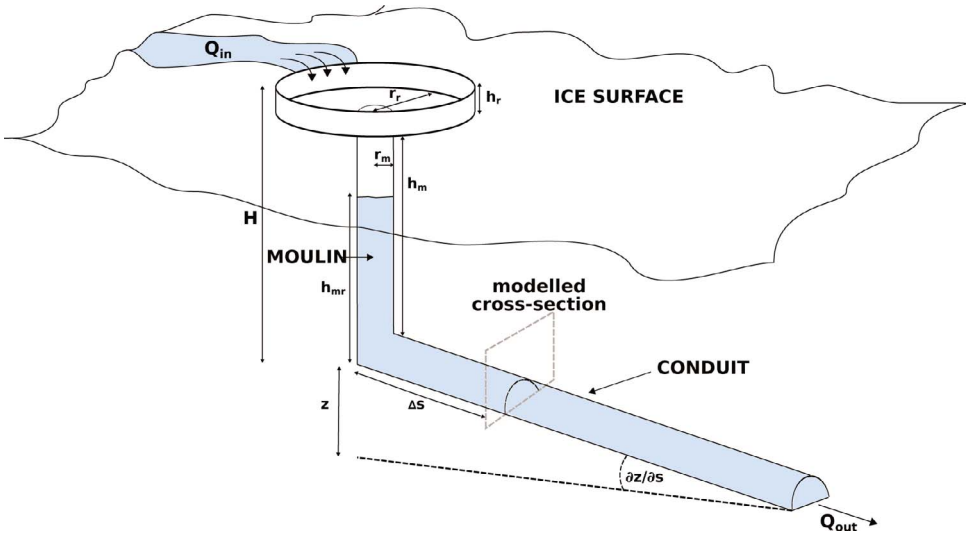

Figure 8. Schematic showing the model configuration. The drawing is not to scale. Symbols are defined in the text.

glacier surface to the ice sheet bed [*Catania and Neumann*, 2010]. The moulin is subject to influx of meltwater from the ice sheet surface and a single, straight conduit, with semi-circular cross section, then drains from the moulin base to the ice margin (Figure 8). The model differs slightly from that used by *Cutler* [1998] in that we do not attempt to account for changes in the shape of the channel cross-section. By employing equation (1), however, we are able to incorporate both cavity and R-channel type behavior [*Schoof*, 2010].

[32] The moulin is considered to be a vertical circular pipe with constant radius, r_m which is fed by a supraglacial stream for which the discharge, Q_{in}, can be prescribed. A reservoir of depth h_r and radius r_r, sits at the top of the moulin and represents a supraglacial pond which allows water to collect at the ice sheet surface if the moulin should overflow. The height of the moulin is then equal to the ice thickness, H, minus h_r at its top, and the channel radius at the moulin base (Figure 8).

[33] Water flow through the conduit is calculated using equation (2). $\frac{\partial \phi}{\partial s}$, which drives water flow, is given by:

$$-\frac{\partial \phi}{\partial s} = \frac{\Delta z}{s} + \frac{\max(h_{mr}, 0)}{s} \tag{3}$$

where z is conduit elevation, h_{mr} is a function of hydraulic head in the moulin/reservoir section of the system and s is the full conduit length. It is assumed that $\frac{\partial \phi}{\partial s}$ is constant along the conduit and that water emerges at the glacier margin at atmospheric pressure.

[34] We use the model to simulate channel cross-section evolution at a distance Δs from the base of the moulin (Figure 8). We assume that ice thickness is constant in the vicinity of the cross-section, negating the effect of local glacier geometry on hydraulic potential [cf. *Shreve*, 1972]. In addition, in this model the conduit rests on bedrock (i.e., no water is lost into a subglacial aquifer) and there is no energy transfer between the water and the channel bed. We also do not account for heat advection along the conduit, which is likely to be minimal, or conduction of heat into cold ice.

[35] At each time step, water volume within the system is determined in accordance with the conservation of mass:

$$\frac{\partial V}{\partial t} = Q_{in} - Q_{out} \tag{4}$$

where V is the total volume of water within the modeled system. This allows us to calculate the hydraulic head within the moulin/reservoir. If there is no water stored in the moulin then open-channel flow occurs and the hydraulic gradient is simply $\frac{\Delta z}{s}$. If no water is backed up in the conduit, Q_{out} falls to be equal to Q_{in}.

[36] When the conduit is full then A is equal to S. In the case of open-channel flow, however, A must be calculated at each time step using the volume of water remaining in the system, V. Equations (1) and (4) are solved numerically using the Matlab ode15s stiff differential equation solver [*Shampine and Reichelt*, 1997], producing time series of the conduit evolution, discharge and pressure characteristics in response to a time-varying water input signal.

[37] The justification for the model structure, where we envisage a single conduit rather than attempting to simulate the evolution of a spatially distributed network [cf. *Schoof*, 2010], is provided by field observations which suggest that delivery of meltwater to the subglacial drainage system from the ice sheet surface typically occurs at discrete locations, through moulins or crevasses. It is likely that a spatially distributed drainage system results from year-round melt-water generation at the ice-bed interface. We suggest that water drainage from a smaller number of discrete points may mean that seasonal development of the subglacial drainage system is concentrated in relatively few conduits and that these newly developed conduits co-exist and interact with the pre-existing distributed system.

[38] Although not explicitly modeled here, interaction between an efficient channel and a wider drainage system has been observed in Alpine glaciers [e.g., *Hubbard et al.*, 1995]. Over-pressurization of a subglacial conduit can set up lateral pressure gradients, driving water away from the conduit and

increasing water pressure in the surrounding drainage system [*Hubbard et al.*, 1995; *Hubbard and Nienow*, 1997]. Since the volume of meltwater produced at the ice sheet surface is more than an order of magnitude greater than is generated at the ice-bed interface, the behavior of these conduits is likely to force, rather than respond to, behavior in the remainder of the system. This suggests, then, that the behavior of a large conduit has the potential to govern more widespread increases in ice velocity [*Fountain*, 1994; *Hubbard et al.*, 1995; *Hubbard and Nienow*, 1997; *Bartholomaus et al.*, 2007; *Palmer et al.*, 2011].

[39] We note that flow concentration is also expected from numerical analysis of subglacial drainage system behavior [*Shreve*, 1972; *Röthlisberger*, 1972; *Schoof*, 2010; *Hewitt*, 2011]. A recent study by *Schoof* [2010], on which our equations are based, models a distributed network of conduits with spatially uniform inputs. In this model efficient R-channels develop during the model run as larger conduits capture water at the expense of smaller ones. The pressure behavior of larger conduits dominates the overall pressure regime [*Schoof*, 2010].

[40] Our model approach contains a number of important assumptions which are introduced for the sake of computational simplicity. First, that the pressure gradient is uniform along the entire conduit. In reality, the effect of glacier geometry and bed elevation, as well as channel morphology, will alter this gradient. In addition, changes in discharge may occur at different points downstream due to additional inputs of meltwater, either at the base of further moulins or confluences with other conduits. Secondly, we prescribe a constant rate of basal sliding, u_b, which contributes to opening of conduits by horizontal motion past bedrock obstacles. A more sophisticated model would couple increases in water pressure with the rate of basal motion through a sliding law, which may alter the point of transition from cavity to R-channel type behavior. In extreme scenarios, such as glacier surges, high enough rates of u_b may act to obliterate subglacial conduits [e.g., *Kamb*, 1987]. It is also assumed that water is able to penetrate straight to the ice bed on entering the moulin, meaning that water can only back up in the moulin if Q_{in} is greater than Q_{out}. Water storage at the ice surface, either in lakes or by filling of crevasses prior to the establishment of a hydraulic connection between the ice surface and its bed, can only be replicated by manually specifying an initial water height in the moulin/reservoir.

[41] In light of these limitations, the purpose of this study is not to provide a comprehensive treatment of subglacial drainage system behavior, nor to tune the model results to fit a set of observations. Rather we hope to assess whether a simple model of subglacial conduit behavior, as it responds to time-varying meltwater input, can reproduce patterns of subglacial water pressure that might explain the features of the seasonal acceleration signal which were described in the first part of this paper.

5.1. Experiment 1: Model Testing

[42] In our first experiment we test the response of the conduit model to a forcing signal which simulates the key features of seasonal meltwater delivery to the subglacial drainage system that were identified in the first part of this paper. The model setup is based on a moulin which is located ~500 m south of site 2. Site 2 is 7.3 km along our transect from the ice sheet margin and the ice thickness is 375 m (Figure 1) [*Bamber et al.*, 2001; *Krabill*, 2010]. Based on field observations of this moulin, values of r_m = 3 m, r_r = 250 m and d_r = 5 m were adopted.

[43] We specify an initial conduit cross-sectional area $S_0 = u_b h/c_2 N n$ and allow the model to spin-up for 5 days with no water inputs, reproducing conditions to represent the state of the conduit following the winter period. The model is run for 100 further days with a meltwater signal which comprises: (i) a seasonal component which peaks at 4 $m^3\ s^{-1}$; (ii) daily cycles in meltwater production, with amplitude of 1 $m^3\ s^{-1}$ which are superimposed on the seasonal signal; and (iii) three pulses of meltwater which last two days each and have peak discharge of 5 $m^3\ s^{-1}$ (Figure 9a). The full list of model parameters is provided in Table 1.

[44] Inspection of Figure 9 indicates that the model is able to reproduce key features of the seasonal subglacial drainage system behavior reasonably well. When water drains into the conduit initially, the small conduit size restricts Q_{out} to be much smaller than Q_{in} and water backs up in the moulin. High water level, which fills the moulin but does not cause the reservoir to overflow, causes high subglacial water pressure and an increase in the hydraulic gradient, $\frac{\partial \phi}{\partial s}$. Increased $\frac{\partial \phi}{\partial s}$ forces higher discharge through the conduit, which leads to rapid growth of the cross-section. A positive feedback between conduit size and discharge then develops, and both Q_{out} and S continue to increase rapidly until the conduit has become large enough to drain all the water stored in the moulin. At this point, which occurs after ~5 days, pressure in the conduit drops rapidly as the meltwater input is not sufficient to fill the expanded conduit. The weight of overlying ice causes the conduit to adjust in size, until S and Q_{in} are more or less in balance after a period of a few days. Following the development of the conduit in response to initial meltwater input, the conduit size continues to adjust to changes in water input and short-term variations in the forcing signal cause large fluctuations in both water pressure and conduit size. This is evident both in response to the diurnal cycles in the meltwater signal, as well as the three pulses which occur on days 15, 30 and 45 (Figure 9).

[45] Short-term changes in water pressure reflect temporary imbalance between the water supply, Q_{in}, and the capacity of the conduit to evacuate the water. The capacity to remove water is governed by equation (2) which states that a larger conduit and increased hydraulic gradient both lead to higher discharge. At the same time, however, increased hydraulic gradient and larger discharge also causes an increase in conduit size. In our model, fluctuations in water pressure occur when the meltwater input signal overfills the conduit more quickly than the rate of wall melting can increase the conduit size in order to accommodate the extra water, leading to the imbalance between Q_{out} and Q_{in}. Under these conditions water is stored in the englacial system increasing the hydraulic gradient and subglacial water pressure. The high pressure lasts until the water supply drops, at which point the conduit is larger than is necessary to evacuate the incoming meltwater and open channel flow occurs while the conduit slowly reduces in size again. The pulse events demonstrate that high water pressure can be sustained in the conduit for periods of more than one day, so long as Q_{in} keeps rising. These events cause the conduit to reach its

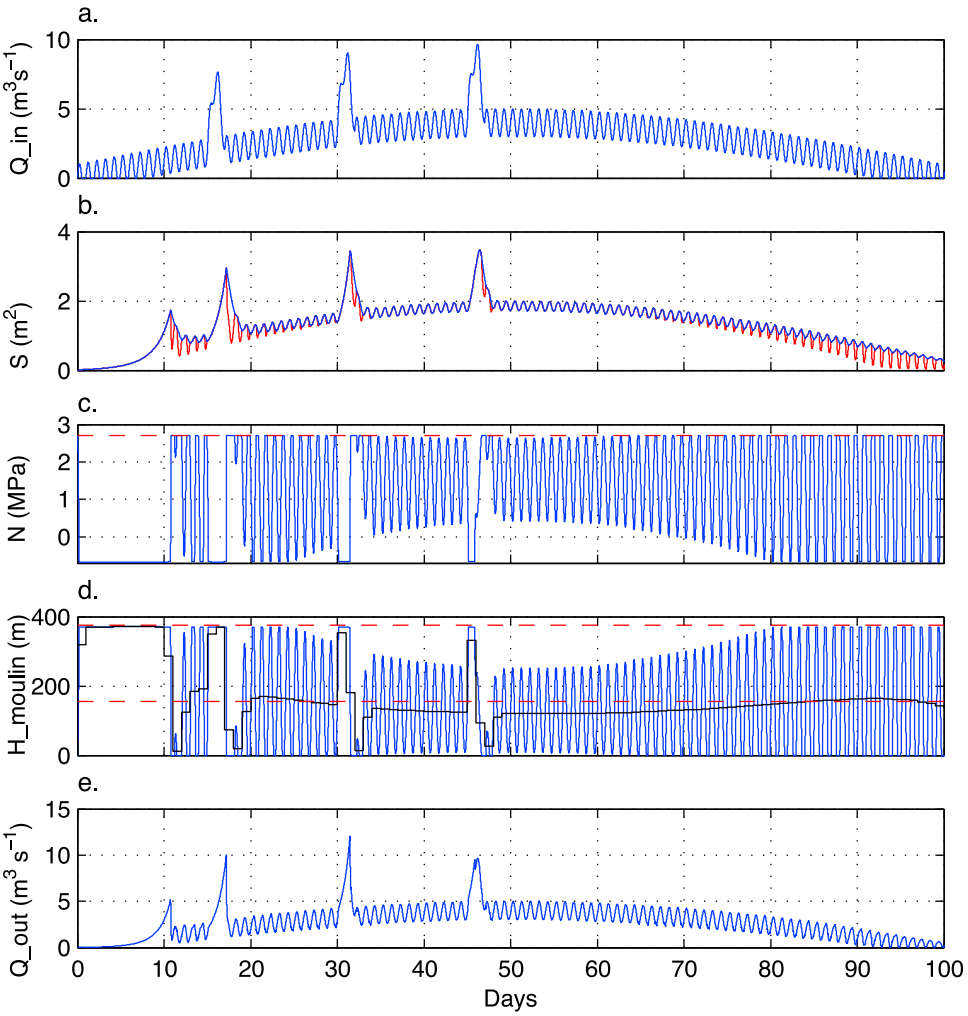

Figure 9. Simulation of channel-cross section evolution in response to a time-varying water input signal. (a) Inflow to the system, Q_{in}. (b) Conduit cross-sectional area, S (blue) and filled cross-sectional area (red) under open-channel conditions. (c) Effective pressure, $N = p_i - p_w$ (blue), at the modeled cross-section. Maximum N is equal to p_i (red dashes). (d) Water height in the moulin/reservoir system (blue), which drives variation in the hydraulic head gradient. Mean water height is shown for 24h periods (black steps) and the whole model run (lowest red dashes). Ice thickness, H is indicated by the upper red dashes. (e) Outflow from the system, Q_{out}.

greatest size and also maintain the highest daily mean water pressures excepting the spring-event. Following the pulse events, however, daily cycles in water pressure are suppressed while the conduit size adjusts more slowly to the reduction in meltwater input.

[46] The conduit response to the seasonal component of the Q_{in} signal, however, is very different. Because Q_{in} varies only gradually on the longer-term the conduit is able to shrink and contract on the same timescales without a sharp rise in water pressure [*Schoof*, 2010]. Running the model with the same parameters, but removing the short-term components of the Q_{in} signal, we find that mean water pressure in the conduit changes steadily with the water supply and is inversely related to Q_{in}. This pressure-discharge relationship is consistent with the behavior of an R-channel in steady state [*Schoof*, 2010].

[47] Diurnal variations in water pressure are greatest at the beginning and end of the model run, when the size of the daily cycles in meltwater supply are greater as a proportion of the daily mean Q_{in} (Figure 9). The same also applies to the pulse events: the first pulse on day 15 achieves the highest water pressure, while the third pulse, which occurs on day 45 near the peak of seasonal water input, is more subdued. This behavior highlights an important link between short-term variations in meltwater input and the longer-term evolution of the conduit. Since the conduit size is broadly in equilibrium with the longer-term signal of meltwater input, S is largest in the middle part of the model run, near the peak of the 'seasonal' signal. The larger channel has greater capacity to evacuate meltwater, therefore more water is required to overfill it and pressurize the conduit than earlier in the season when the conduit was smaller. In this way, the ratio between mean Q_{in} and the rate and magnitude of short-term changes in Q_{in} controls the magnitude of short-term spikes in water pressure within the conduit. Overall, this suggests that a larger seasonal meltwater input signal may act to limit the

Table 1. Parameter Values Used During the Model Experiments[a]

Parameter	Symbol	Value	Units
Ice thickness at the moulin	H	375	m
Moulin radius	r_m	3	m
Reservoir radius	r_r	250	m
Reservoir depth	h_r	5	m
Conduit slope	$\frac{\partial z}{\partial s}$	0.02	-
Conduit length	s	7300	m
Distance of cross-section from moulin	Δs	500	m
Melt opening parameter	c_1	$\frac{1}{\rho_i L}$	-
Darcy-Weisbach friction factor	f	0.2	-
Latent heat of fusion	L	3.35×10^5	J kg^{-1}
Density of water	ρ_w	1000	kg m^{-3}
Density of ice	ρ_i	910	kg m^{-3}
Glen's flow law coefficient	B	5.3×10^{-24}	Pa^{-3} s^{-1}
Glen's flow law exponent	n	3	-
Conduit closure parameter	c_2	$2Bn^{-n}$	-
Basal sliding velocity	u_b	30	m yr^{-1}
Bedrock obstacle height	h	0.1	m

[a]The parameters reflect plausible field conditions and commonly used values for ice temperate ice [e.g., *Paterson*, 1994].

size of short-term variations in water pressure while larger short-term variations in meltwater supply, relative to mean meltwater input, would favor greater changes in water pressure.

[48] The preceding discussion suggests that key features of the subglacial drainage system response to inputs of meltwater from the ice sheet surface may be explained in terms of time-varying water input to a subglacial conduit without invoking the transition from cavity to R-channel type steady state behavior. For a full semicircular conduit, *Schoof* [2010] derived the following equation for the critical discharge value at which a switch from cavity to R-channel type behavior in steady state would occur:

$$Q_c = \frac{u_b h}{c_1(1-\alpha)\frac{\partial \phi}{\partial s}} \tag{5}$$

where $\alpha = 5/4$ is a constant. Under full and steady state conditions, assuming a fixed hydraulic gradient, the critical discharge for the conduit modeled here is 0.59 m^3 s^{-1}, which corresponds to a cross-sectional area of 0.16 m^2. Our model suggests, therefore, that the Q_c is easily exceeded very early in the initial growth phase. Figure 9 shows, however, that water pressure continues to rise during the spring-event even once the conduit has become 'channelized'.

[49] Overall, this set of simulations suggests that the subglacial conduit does not reach steady state with an input signal which varies on such short timescales. This results in short-term pressure variations within the conduit, which, should high pressure in the conduit cause increases in pressure over a wider area by interaction with a distributed drainage system, could plausibly integrate to explain the seasonal velocity signal observed at sites 1–3 in the first part of the paper.

5.2. Experiment 2: Forcing With Realistic Input Signal

[50] We now use field observations of temperature and surface ablation from site 2 in 2010 to generate a more realistic meltwater signal to drive conduit evolution. Runoff was estimated using a simple temperature-melt index model [*Hock*, 2003] applied to a 1 × 3 km rectangular catchment with a surface gradient of 0.025. This estimated catchment area is based on field observations of the spacing of moulins in the Leverett Glacier catchment during traverses by helicopter and on foot, and on observations of mean discharge into moulins at this elevation. The surface gradient was calculated using surface elevation data from a recent airborne survey (Figure 1) [*Krabill*, 2010]. A measurement of seasonal surface ablation was then used to calculate a degree-day factor of 0.012 m °C^{-1} d^{-1} for the period 1 May–1 August [*Hock*, 2003]. Applying a fixed lapse rate of −0.9°C per 100 m elevation, calculated using temperature from sites 2 and 3 in May and June, we then used the temperature data to estimate runoff for a period of 92 days, from 1 May until 1 August, at which point the temperature sensor at site 2 failed. Using this input signal, we find that the diurnal variations in the response are quite subdued, and we therefore artificially amplify the daily signal in this runoff estimate by a factor of 2. This is justified somewhat, recalling that the temperature index is itself only an approximation to the average runoff, and additional factors likely control the variability of runoff into the moulins. We ran the conduit model, following spin-up, from May 1st until August 1st and conduit evolution was driven by the estimated runoff signal (Figure 10a).

[51] Running the model with this meltwater signal results in similar conduit behavior to that modeled in response to the artificial signal (Figures 9 and 10). A period of high subglacial water pressure and rapid conduit growth occurs when water first drains into the conduit. Following this, water pressure drops and the conduit reduces in size. For the rest of the melt season, the conduit continues to evolve in response to short-term variations in meltwater input. This is evident both in daily cycles in water pressure and conduit growth as well as longer-term periods of increased meltwater input, on the order of a few days, which sustains higher water pressures for longer and marked conduit growth. For example, a period of higher meltwater input from 22–28 May causes the conduit to reach its greatest size and high mean water pressure is sustained for 3–4 days. Daily cycles in water pressure, where the conduit high pressure occurs during the day and is reduced when meltwater input starts to fall, are persistent for most of the model run.

[52] As with the velocity observations presented in the first part of this paper, there is no clear relationship between the magnitude of daily cycles in the input signal and the pressure response within the subglacial conduit. We suggest that this reflects the strong time-dependence of the relationship between meltwater supply and subglacial water pressure. For example, if larger diurnal variations in meltwater supply increase the size of the conduit, it will be over-filled for a shorter period of the day and require greater amounts of water to achieve the same water pressure. In this way the water pressure is highly sensitive to the recent development of the system.

[53] Comparing the modeled conduit development with the observed velocity record from site 2 (Figure 10c) yields striking results which support our conceptual model. High ice velocities are well matched with growth of the conduit, which is indicative of sustained high water pressure. The highest velocities coincide with sharpest rises in conduit cross-sectional area and begin to reduce again when water input declines and the conduit shrinks in size. Over daily

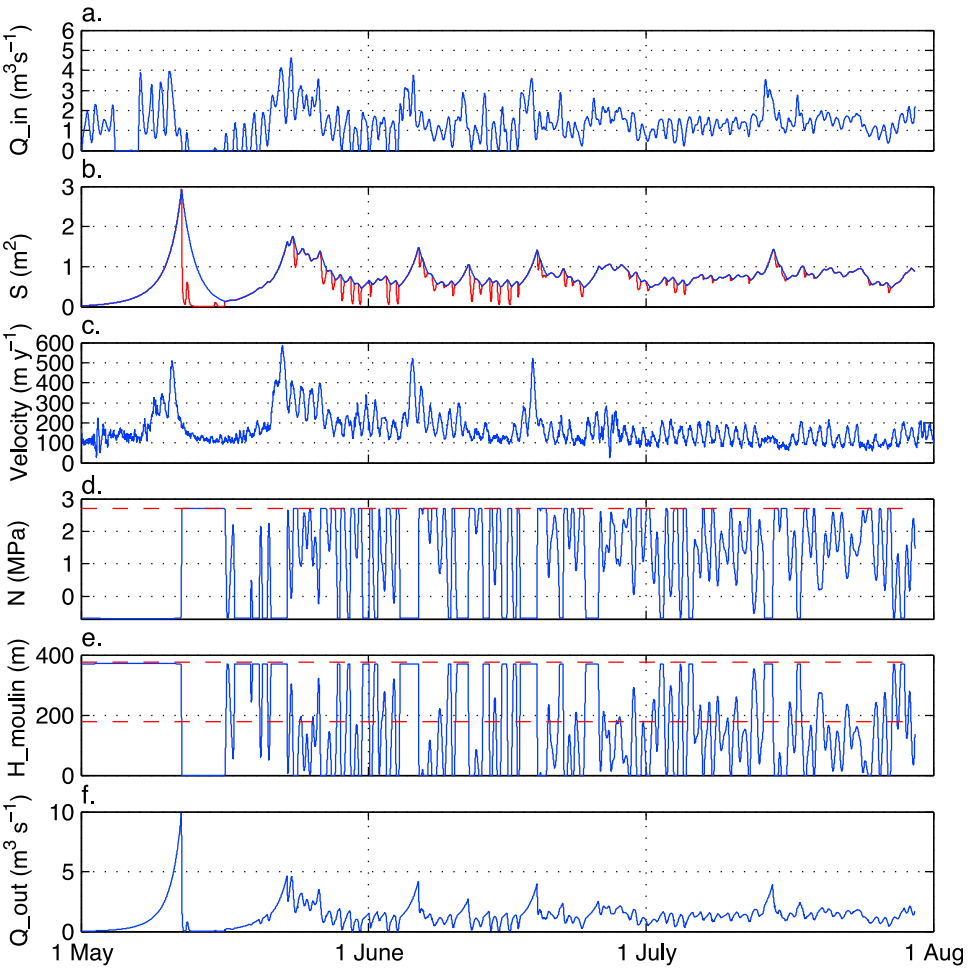

Figure 10. Simulation of channel-cross section evolution in response to a realistic water input signal generated from temperature data at site 2 in 2010, compared with the record of ice velocity. (a) Inflow to the system, Q_{in}. (b) Conduit cross-sectional area, S (blue) and filled cross-sectional area (red) under open-channel conditions. (c) Ice velocity at site 2 during the 2010 summer melt season. (d) Effective pressure, $N = p_i - p_w$ (blue), at the modeled cross-section. Maximum N is equal to p_i (red dashes). (e) Water height in the moulin/reservoir system (blue), which drives variation in the hydraulic head gradient. Mean water height is shown for 24h periods (black steps) and the whole model run (lowest red dashes). Ice thickness, H is indicated by the upper red dashes. (f) Modeled outflow from the system, Q_{out}.

timescales, high velocity occurs when the channel is overfilled and low velocities, which often return to winter background levels, occur during periods of open-channel flow.

[54] In common with the previous experiments, the conduit reaches R-channel size during the spring-event and remains above the critical value through the remainder of the model run. After the spring-event Q_{out} roughly matches Q_{in} suggesting longer-term variability in meltwater input is more easily accommodated by evolution of the conduit.

6. Discussion

[55] The field data show that changes in ice velocity, and therefore presumably water pressure in the subglacial drainage system, are roughly in phase with meltwater discharge from the Leverett Glacier snout over short timescales. Both variations in temperature and periodic drainage of meltwater which has accumulated at the ice sheet surface can cause ice acceleration by raising meltwater input to the drainage system over a period of a few days. Daily cycles in ice velocity also appear to be forced by increased meltwater flux through the subglacial drainage system. Although we cannot unequivocally resolve daily cycles in the surface uplift record, we argue that the sheer magnitude of these velocity variations suggests that they are forced locally and are not due to coupling to ice further downglacier.

[56] Over the full melt-season, however, we do not find a consistent positive relationship between ice velocity and meltwater discharge. Mean ice velocities are lower in late summer, following peak discharge, than in early summer. If we assume that the subglacial drainage system is distributed and inefficient prior to the initial spring acceleration, following the winter period, this observation indicates that the drainage system becomes channelized at some point during the melt season, and that this limits the overall summer acceleration [*Bartholomew et al.*, 2010, 2011a; *Sundal et al.*, 2011].

[57] Inspection of the detailed structure of the ice velocity records from sites 1–3 reveals that the discrepancy between early and late summer velocities is due to the absence of multiday speed-up events in the latter part of the summer melt season. They dominate the early season velocity records but do not appear once discharge has peaked and/or stabilized, while daily cycles in ice velocity are evident through most of the melt season (Figures 2 and 4). In late summer, therefore, either the meltwater input signal which forces short-term variations in ice motion is different from early summer, or the drainage system has developed to become less responsive to the same forcing.

[58] Two observations suggest the former. First, multiday events are associated with steep rises in proglacial discharge which are largely absent in the late season. The hydrological study from this catchment in 2009 showed that an efficient subglacial drainage system expands upglacier from the ice sheet margin, at the expense of the inefficient winter drainage configuration, in response to inputs of meltwater from higher elevations as the melt season progresses [*Bartholomew et al.*, 2011b]. Increasing proglacial discharge therefore represents not only increasing temperatures, but an expanding area of the ice sheet surface from which meltwater is delivered, via the subglacial drainage system, to the ice sheet margin. Hydrological parameters such as ion-concentration and suspended sediment concentration also indicate that this process results in continued evolution of the drainage system until the catchment reaches its full inland extent (presumably meltwater from higher elevations drains through a different outlet glacier), at which point the drainage system reaches a more stable state [*Bartholomew et al.*, 2011b]. We suggest, therefore, that the multiday events on the rising limb of discharge are the consequence of pressure increases in a subglacial drainage system which is continually expanding to accommodate extra sources of meltwater. Once the drainage system has fully expanded, the discharge becomes more stable and these events are less likely to occur. Secondly, the large daily cycles indicate that velocity *is* still responsive to variations in meltwater input on a short-term basis, even once the subglacial drainage system has become channelized. This suggests that large pulses of meltwater, derived from increased surface melting over a wider area or drainage of stored supraglacial water, would still have the capacity to cause a large increase in ice velocity should they occur.

[59] The observations from sites 1–3 are not easily explained using a binary interpretation of subglacial drainage system which is inferred by steady state analyses of drainage system behavior [cf. *Sundal et al.*, 2011]. Preliminary dye-tracing experiments performed in 2010 indicate that fast (channelized) drainage conditions exist between site 2 and the ice sheet margin on May 31st, and from 14 km along the transect on June 2nd. Ice velocities at site 2 exceeded 500 m yr^{-1} on June 5th and 18th of that summer, however, during the peaks of two separate multiday acceleration events. This indicates that transition from a slow (distributed) to channelized drainage system does not prevent the large multiday events which our data have revealed and is not the cause for the difference between early and late summer velocities. As discharge into the system increases, subglacial channels will get larger and more water will be required to over-pressurize them. Since this effect is not pronounced in our data set, however, variability in meltwater forcing appears to exert greater control on changes in ice velocity.

[60] At higher elevation sites, the pattern of sporadic high velocity events, superimposed on slightly raised background velocity, suggests a cycle of intermittent local drainage events [*Das et al.*, 2008] which overwhelm the subglacial drainage system, combined with steady drainage to the ice-bed interface and coupling to faster moving ice downglacier [*Price et al.*, 2008]. Diurnal variation in meltwater delivery to moulins at higher elevation sites is likely to be muted because moulins are spaced further apart and the snowpack remains for most of the summer making supraglacial travel times very long [*Nienow and Hubbard*, 2006; *Campbell et al.*, 2006]. In the longer-term, following initial drainage of meltwater to the ice-bed interface, steady delivery of meltwater to the subglacial drainage means that the capacity of the system is in balance with inputs and short-term over-pressurization (and therefore ice acceleration) is less likely to occur.

[61] Our data do not show whether the drainage system beneath higher elevation sites becomes channelized following initial drainage of meltwater. Although thicker ice increases creep closure rates in subglacial conduits, supraglacial streams can be large (>5 m^3 s^{-1}) and could conceivably maintain efficient conduits. Even if an efficient system cannot be sustained, however, lower ice velocities might be explained because the forcing is not great enough to raise water pressure over a wide enough area to have a significant impact on ice velocity [e.g., *Iken and Bindschadler*, 1986; *Iken and Truffer*, 1997]. The presence of daily cycles in ice velocity at site 5 in 2010 appears, therefore, to be caused by higher rates of surface melting. This favors early removal of the snowpack, allowing greater diurnal variability in meltwater supply to moulins. In addition, higher volumes of meltwater are also able to over-pressurize the drainage system more easily.

[62] The agreement between our simple model of subglacial conduit development and observations of ice velocity provides justification for the model structure. The results suggest that the behavior of an efficient subglacial drainage channel, fed by meltwater from the ice sheet surface, can effectively govern subglacial water pressures over a wider area [*Kamb et al.*, 1994; *Hubbard et al.*, 1995; *Hubbard and Nienow*, 1997; *Nienow et al.*, 2005]. Ice velocities are raised when meltwater drainage into the system rises more quickly than conduits can expand to accommodate the extra water. This is likely to occur through lateral pressure gradients which drive water away from the conduit and increase water pressure in the surrounding drainage system when the main conduit becomes overfilled [*Hubbard et al.*, 1995; *Hubbard and Nienow*, 1997]. The rapid changes in both modeled water pressure and observed ice velocity suggest further that the timescales for water pressure diffusion into the surrounding drainage system are relatively short [*Hubbard et al.*, 1995; *Hewitt*, 2011].

[63] The prevalence of short-term variations in ice velocity suggests very strongly that steady state conditions rarely occur in practice in this section of the GrIS margin. We contend, then, that the difference between our results and the recent modeling study by *Schoof* [2010] is simply due to the variability in meltwater drainage that we observe in our data. In light of these findings we argue that it is important to

consider the unsteady growth of the drainage system, regardless of whether it is channelized or otherwise, rather than relying on a binary characterization of its behavior based on steady state analysis.

[64] Previous studies from this transect have shown that increased summer ablation does not necessarily lead to a reduction in annual ice velocities [*Bartholomew et al.*, 2011a]. Our investigation substantiates the arguments put forward that variability in the *rate*, rather than absolute volume, of meltwater delivery to the subglacial drainage system is an important control on patterns of subglacial water pressure. In a warmer climate, therefore, we would expect the summer acceleration signal at lower elevations to be sustained by variability in meltwater delivery to the ice-bed interface, particularly in early summer while the system is continually adjusting to larger and larger inputs of meltwater.

[65] Behavior at higher elevations, where overall seasonal acceleration is lower, appears to be controlled strongly by supraglacial and englacial hydrology. In the first instance, accumulation and sudden drainage of stored water from the ice sheet surface control the timing of hydrologically forced ice acceleration [*Bartholomew et al.*, 2011a]. Two previous studies have shown that higher melt rates result in greater seasonal increases in ice motion because meltwater can drain to the ice-bed interface earlier in the season, increasing the time for velocity variations to occur [*Bartholomew et al.*, 2011a]. Following the initial drainage event, long supraglacial transit times mean that short-term cycles in meltwater inputs to the ice sheet bed are subdued. When there is more meltwater, however, the input signal can vary more quickly over shorter timescales and the record at site 5 shows that the behavior of higher elevation sites becomes more like those nearer the ice sheet margin. At these sites, a warmer climate therefore favors greater seasonal acceleration on two counts, by increasing the length of time for which meltwater can reach the bed, and by increasing the short-term variability in that supply.

7. Conclusions

[66] High resolution measurements of ice velocity in a land-terminating section of the GrIS reveal that the seasonal ice velocity signal is dominated by short-term variations in ice velocity. These short-term variations in ice velocity are forced by rapid variations in meltwater input to the subglacial drainage system from the ice sheet surface. The absence of short-term cycles in ice velocity at higher elevation sites reflects different patterns of meltwater input to the ice-bed interface, which are controlled by supraglacial and englacial hydrology. At these sites the velocity signal reflects more gradual variations in meltwater input, punctuated by events where large volumes of stored meltwater drain to the ice-bed interface.

[67] We find that an efficient drainage system is likely to be established shortly after initial access of meltwater to the ice bed interface, which occurs at progressively higher elevations through the melt season. Large velocity variations can continue to occur, however, even once the drainage system has become channelized. Using a simple model of subglacial conduit behavior we show that the record can be understood in terms of a time-varying water input to a channelized subglacial drainage system. Our investigation substantiates the arguments that variability in the *rate*, rather than absolute volume, of meltwater delivery to the subglacial drainage system is an important control on patterns of subglacial water pressure. These findings help explain the failure of steady state analyses of subglacial drainage system behavior to explain inter-annual variations in summer ice velocity in this part of the GrIS margin.

[68] In the context of predictions about the impact of increased meltwater production on ice dynamics and therefore on the future mass balance of the GrIS, we find no evidence to suggest a reduction in summer ice velocity at sites near the ice sheet margin where water easily drains to the ice bed interface. At sites further inland, increased rates of surface melting favors greater summer acceleration both because water will drain to the ice-bed interface earlier each year and earlier snowpack removal will lead to greater melt supply variability. Overall, our findings provide new insight into the role that the subglacial drainage system plays in moderating the relationship between surface melting and ice velocity [cf. *Van de Wal et al.*, 2008; *Shepherd et al.*, 2009; *Schoof*, 2010; *Sundal et al.*, 2011; *Pimentel and Flowers*, 2011].

[69] **Acknowledgments.** We thank for financial support: UK Natural Environment Research Council (NERC, through studentships to I.B./T.C. and grants to P.N./D.M.), Edinburgh University Moss Centenary Scholarship (I.B.), the Carnegie Trust (through a Research Grant to P.N.). GPS equipment and training were provided by the NERC Geophysical Equipment Facility. M.A.K. was funded by a RCUK Academic Fellowship.

References

Anderson, R., S. Anderson, K. MacGregor, E. Waddington, S. O'Neel, C. Riihimaki, and M. Loso (2004), Strong feedbacks between hydrology and sliding of a small alpine glacier, *J. Geophys. Res.*, *109*, F03005, doi:10.1029/2004JF000120.

Bamber, J., R. Layberry, and S. Gogineni (2001), A new ice thickness and bed data set for the Greenland ice sheet: I. Measurement, data reduction, and errors, *J. Geophys. Res.*, *106*, 33,773–33,780, doi:10.1029/2001JD900054.

Bartholomaus, T., R. Anderson, and S. Anderson (2007), Response of glacier basal motion to transient water storage, *Nat. Geosci.*, *1*, 33–37.

Bartholomew, I., P. Nienow, D. Mair, A. Hubbard, M. King, and A. Sole (2010), Seasonal evolution of subglacial drainage and acceleration in a Greenland outlet glacier, *Nat. Geosci.*, *3*, 408–411.

Bartholomew, I., P. Nienow, A. Sole, D. Mair, T. Cowton, S. Palmer, and M. King (2011a), Seasonal variations in Greenland Ice Sheet motion: Inland extent and behaviour at higher elevations, *Earth Planet. Sci. Lett.*, *307*, 271–278, doi:10.1016/j.epsl.2011.04.014.

Bartholomew, I., P. Nienow, A. Sole, D. Mair, T. Cowton, S. Palmer, and J. Wadham (2011b), Supraglacial forcing of subglacial hydrology in the ablation zone of the Greenland Ice Sheet, *Geophys. Res. Lett.*, *38*, L08502, doi:10.1029/2011GL047063.

Bingham, R., A. Hubbard, P. Nienow, and M. Sharp (2008), An investigation into the mechanisms controlling seasonal speedup events at a High Arctic glacier, *J. Geophys. Res.*, *113*, F02006, doi:10.1029/2007JF000832.

Campbell, F., P. Nienow, and R. Purves (2006), Role of the supraglacial snowpack in mediating meltwater delivery to the glacier system as inferred from dye tracer investigations, *Hydrol. Processes*, *20*(4), 969–985.

Catania, G. A., and T. A. Neumann (2010), Persistent englacial features in the Greenland Ice Sheet, *Geophys. Res. Lett.*, *37*, L02501, doi:10.1029/2009GL041108.

Chen, G. (1999), GPS kinematic positioning for the airborne laser altimetry at Long Valley, California, PhD thesis, Mass. Inst. of Tech, Cambridge.

Clarke, G. (1996), Lumped-element analysis of subglacial hydraulic circuits, *J. Geophys. Res.*, *101*, 17,547–17,559, doi:10.1029/96JB01508.

Clarke, G. (2003), Hydraulics of subglacial outburst floods: New insights from the Spring-Hutter formulation, *J. Glaciol.*, *49*(165), 299–313.

Cutler, P. (1998), Modelling the evolution of subglacial tunnels due to varying water input, *J. Glaciol.*, *44*(148), 485–497.

Das, S., I. Joughin, M. Behn, I. Howat, M. King, D. Lizarralde, and M. Bhatia (2008), Fracture propagation to the base of the Greenland Ice Sheet during supraglacial lake drainage, *Science*, *320*(5877), 778–781.

Fountain, A. (1994), Borehole water-level variations and implications for the subglacial hydraulics of South Cascade Glacier, Washington State, USA, *J. Glaciol.*, *40*(135), 293–304.

Herring, T., R. King, and S. McClusky (2010), *Documentation for the GAMIT GPS Analysis Software, Version 10.4*, Mass. Inst. of Tech., Cambridge, Mass.

Hewitt, I. (2011), Modelling distributed and channelized subglacial drainage: The spacing of channels, *J. Glaciol.*, *57*(202), 302–314.

Hock, R. (2003), Temperature index melt modelling in mountain areas, *J. Hydrol.*, *282*(1–4), 104–115.

Hooke, R., P. Calla, P. Holmlund, M. Nilsson, and A. Stroeven (1989), A 3 year record of seasonal variations in surface velocity, Storglaciaren, Sweden, *J. Glaciol.*, *35*(120), 235–247.

Hubbard, B., and P. Nienow (1997), Alpine subglacial hydrology, *Quat. Sci. Rev.*, *16*(9), 939–955.

Hubbard, B., M. Sharp, I. Willis, M. Nielsen, and C. Smart (1995), Borehole water-level variations and the structure of the subglacial hydrological system of Haut Glacier d'Arolla, Valais, Switzerland, *J. Glaciol.*, *41*(139), 572–583.

Iken, A. (1981), The effect of the subglacial water pressure on the sliding velocity of a glacier in an idealized numerical model, *J. Glaciol.*, *27*(97), 407–421.

Iken, A., and R. Bindschadler (1986), Combined measurements of subglacial water pressure and surface velocity of Findelengletscher, Switzerland: conclusions about drainage system and sliding mechanism, *J. Glaciol.*, *32*(110), 101–119.

Iken, A., and M. Truffer (1997), The relationship between subglacial water pressure and velocity of Findelengletscher, Switzerland, during its advance and retreat, *J. Glaciol.*, *43*(144), 328–338.

Iken, A., H. Rothlisberger, A. Flotron, and W. Haeberli (1983), The uplift of Unteraargletscher at the beginning of the melt season, a consequence of water storage at the bed?, *J. Glaciol.*, *29*(101), 28–47.

Joughin, I., S. Das, M. King, B. Smith, I. Howat, and T. Moon (2008), Seasonal Speedup Along the Western Flank of the Greenland Ice Sheet, *Science*, *320*(5877), 781–783.

Kamb, B. (1987), Glacier surge mechanism based on linked cavity configuration of the basal water conduit system, *J. Geophys. Res.*, *92*, 9083–9100, doi:10.1029/JB092iB09p09083.

Kamb, B., C. Raymond, W. Harrison, H. Engelhardt, K. Echelmeyer, N. Humphrey, M. Brugman, and T. Pfeffer (1985), Glacier surge mechanism: 1982–1983 surge of Variegated Glacier, Alaska, *Science*, *227*(4686), 469–479.

Kamb, B., H. Engelhardt, M. Fahnestock, N. Humphrey, M. Meier, and D. Stone (1994), Mechanical and hydrologic basis for the rapid motion of a large tidewater glacier: 2. Interpretation, *J. Geophys. Res.*, *99*, 15,231–15,244, doi:10.1029/94JB00467.

Krabill, W. (2010), IceBridge ATM L2 Icessn Elevation, Slope, and Roughness, [8.5.2010], http://nsidc.org/data/ilatm2.html, Natl. Snow and Ice Data Cent., Boulder, Colo.

Mair, D., P. Nienow, I. Willis, and M. Sharp (2001), Spatial patterns of glacier motion during a high-velocity event: Haut Glacier d'Arolla, Switzerland, *J. Glaciol.*, *47*(156), 9–20.

Meehl, G., et al. (2007), Global climate projections, in *Climate Change 2007: The Physical Science Basis: Working Group I Contribution to the Fourth Assessment Report of the IPCC*, edited by S. Solomon et al., pp. 747–846, Cambridge Univ. Press, New York.

Nienow, P., and B. Hubbard (2006), Surface and englacial drainage of glaciers and ice sheets, in *Encyclopedia of Hydrological Sciences*, pp. 2568–2575, John Wiley, Hoboken, N. J.

Nienow, P., M. Sharp, and I. Willis (1998), Seasonal changes in the morphology of the subglacial drainage system, Haut Glacier d'Arolla, Switzerland, *Earth Surf. Processes Landforms*, *23*(9), 825–843.

Nienow, P., A. Hubbard, B. Hubbard, D. Chandler, D. Mair, M. Sharp, and I. Willis (2005), Hydrological controls on diurnal ice flow variability in valley glaciers, *J. Geophys. Res.*, *110*, F04002, doi:10.1029/2003JF000112.

Palmer, S., A. Shepherd, P. Nienow, and I. Joughin (2011), Seasonal speedup of the Greenland Ice Sheet linked to routing of surface water, *Earth Planet. Sci. Lett.*, *302*, 423–428.

Parizek, B. (2010), Glaciology: Sliding to Sea, *Nat. Geosci.*, *3*(6), 385–386.

Parizek, B., and R. Alley (2004), Implications of increased Greenland surface melt under global-warming scenarios: Ice-sheet simulations, *Quat. Sci. Rev.*, *23*(9–10), 1013–1027.

Paterson, W. (1994), *The Physics of Glaciers*, Pergamon, Tarrytown, N. Y.

Pimentel, S., and G. Flowers (2011), A numerical study of hydrologically driven glacier dynamics and subglacial flooding, *Proc. R. Soc. A*, *467*(2126), 37–558, doi:10.1098/rspa.2010.0211.

Price, S., A. Payne, G. Catania, and T. Neumann (2008), Seasonal acceleration of inland ice via longitudinal coupling to marginal ice, *J. Glaciol.*, *54*(185), 213–219.

Raymond, C., R. Benedict, W. Harrison, K. Echelmeyer, and M. Sturm (1995), Hydrological discharges and motion of Fels and Black Rapids Glaciers, Alaska, USA: Implications for the structure of their drainage systems, *J. Glaciol.*, *41*(138), 290–304.

Röthlisberger, H. (1972), Water pressure in intra- and subglacial channels, *J. Glaciol.*, *11*(62), 177–203.

Röthlisberger, H., and H. Lang (1987), Glacial hydrology, in *Glacio-fluvial Sediment Transfer: An Alpine Perspective*, edited by A. Gurnell and M. Clark, pp. 207–274, Wiley, Chichester, U. K.

Schoof, C. (2010), Ice-sheet acceleration driven by melt supply variability, *Nature*, *468*(7325), 803–806.

Shampine, L., and M. Reichelt (1997), The Matlab ODE suite, *SIAM J. Sci. Comput.*, *18*(1), 1–22.

Shepherd, A., A. Hubbard, P. Nienow, M. King, M. McMillan, and I. Joughin (2009), Greenland Ice Sheet motion coupled with daily melting in late summer, *Geophys. Res. Lett.*, *36*, L01501, doi:10.1029/2008GL035758.

Shreve, R. (1972), Movement of water in glaciers, *J. Glaciol.*, *11*(62), 205–214.

Sole, A., P. Nienow, I. Bartholomew, D. Mair, T. Cowton, M. King, and M. Burke (2010), Seasonal acceleration of the Greenland Ice Sheet in contrasting melt-seasons, Abstract C42A-02 presented at 2010 Fall Meeting, AGU, San Francisco, Calif., 13–17 Dec.

Spring, U. (1980), *Intraglazialer Wasserabfluss, Theorie und Modellrechnungen*, *Hydrol. und Glaziologie an der Eidgenössischen Tech. Hochsch. Zürich*, vol. 48, Vers. für Wasserbau, Hydrol. und Glaziologie, Zürich, Switzerland.

Sundal, A., A. Shepherd, P. Nienow, E. Hanna, S. Palmer, and P. Huybrechts (2011), Melt-induced speed-up of Greenland Ice Sheet offset by efficient subglacial drainage, *Nature*, *469*(7331), 521–524.

Van de Wal, R., W. Greuell, M. van den Broeke, C. Reijmer, and J. Oerlemans (2005), Surface mass-balance observations and automatic weather station data along a transect near Kangerlussuaq, West Greenland, *Ann. Glaciol.*, *42*, 311–316.

Van de Wal, R., W. Boot, M. Van den Broeke, C. Smeets, C. Reijmer, J. Donker, and J. Oerlemans (2008), Large and rapid melt-induced velocity changes in the ablation zone of the Greenland Ice Sheet, *Science*, *321*(5885), 111–113.

Walder, J. (1986), Hydraulics of subglacial cavities, *J. Glaciol.*, *32*(112), 439–445.

Zwally, H., W. Abdalati, T. Herring, K. Larson, J. Saba, and K. Steffen (2002), Surface melt-induced acceleration of Greenland ice-sheet flow, *Science*, *297*(5579), 218–222.